EFFECT OF SILICATE TREATMENT ON THE CORROSION BEHAVIOR OF HOT-DIP GALVANIZED STEEL.

***Sayed, S. Y.*[*]; Barakat, Y. F.*[*,§]; Abd-El-wahab, S. M.*[†] *and Hassan, H. H.*[†]**

[*] *Tabbin Institute for Metallurgical Studies - P.O. Box 109 Helwan, Cairo, Egypt.*

[†] *Chemistry Dept., Fac. of Science, Ain Shams Univ., Abbasiya, Cairo, Egypt, 11566.*

[§] *Corresponding authors: e-mail addresses: yfbarakat@hotmail.com*

ABSTRACT

Passivation treatment by Potassium silicate solution is considered as an alternative to Chromate conversion treatment to improve the corrosion resistance of hot-dip galvanized steel. One of the main objectives of this study is to evaluate the viability of a simple and industrially easy-to-implement substitute to the widely employed chromate coatings. In this paper, silicate conversion coatings were prepared by immersing hot dip galvanized steel sheets immediately upon removing from the molten zinc in potassium silicate solution bath with chemical composition: 25% SiO_2, 12% K_2O and 63% water, at metal immersion temperatures in excess of about 150°C or higher, the immersion time was constant about 30 s. After optimization of silicate immersion bath concentration and immersion temperature of hot-dip galvanized steel, the corrosion behavior of hot-dip galvanized steel was evaluated by means of electrochemical impedance spectroscopy measurements and Potentiodynamic polarization. The morphology and the phase analysis of zinc-silicate coating were observed by scanning electron microscopy and X-rays diffraction, respectively. The results showed that: the corrosion resistance increased with increasing silicate ions concentration up to 6%, also corrosion resistance increased as temperature of galvanized steel sheet increased up to 250°C. This can be related to the addition of the silicon ions in the zinc coating to form a zinc-silicate complex, which is highly resistant to corrosion.

Keywords: Corrosion, hot-dip galvanized steel, silicate, impedance.

1. INTRODUCTION

Hot-dip galvanizing steel (HDGS) has many useful properties as corrosion resistance, superior mechanical properties, and low maintenance costs that are suitable for widely applications such as automobiles, transportation and construction structures, etc. [1-3]. However, the dissolution rate of zinc is higher than that of steel due to the large potential difference between the steel substrate and zinc layer [4-6].

Among many corrosion protection methods, passivation post treatment is a very important method. Hexavalent chromium or chromate conversion coating is currently the most effective way to inhibit corrosion of metals especially galvanized steel, due to its self-healing nature and corrosion resistance property. However, the use of chromates and other chromium containing compounds has been limited due to their toxicity and carcinogenic effects [7-10]. To cope with this problem, there is a great need to derive new protective coatings yielding not only anticorrosive properties but also friendly to environment. Many attempts have been made to find alternatives, such as phosphating [11, 12], molybdating [13, 14], rare earth salt treatment [15-17] and silicate treatment

[6, 18-23] as well as organic layers such as acrylate [24] ,epoxy resin [25] and silane [26, 27].

Many studies showed that silicate provides environmental friendly and good corrosion resistant coatings for the HDGS [28-33]. The deposition of silicate or silica coatings onto galvanized steels [21, 30, 31, 33-36] has been extensively investigated. It has been reported that for zinc protection with silicate coating, the interfacial region consisted of a zinc silicate layer followed by a layer mainly containing silicate [23, 37]. F. Jamaliet al. [36] proposed that the silicate coating on galvanized steel could effectively inhibit zinc dissolution. The properties of the silicate coating were related to the solution characteristics. Araaki [38] reported that sodium silicate ($Na_2Si_2O_5$) is remarkably effective on zinc dissolution, exhibiting high inhibition efficiencies around 90%. Parashar et al. [39] have reported that the properties of the silicate coatings are directly proportional to the ratio of silica to alkali metal oxide. Yuan et al. [34] have reported that the most compact coating with the best anticorrosion performance was obtained by treatment of HDGS with silicate solution with a molar ratio of 3.5. Dalbin et al. [33] reported that the immersion of electrogalvanized sheets in the silica/silicate immersion bath, which was obtained by mixing silica sol with sodium silicate., produced a more compact coating with better corrosion resistance. F. Jamali et al. [36] study the effect of nano-silica on the corrosion behavior of silicate conversion coatings on HDGS. The results revealed that, potassium silicate conversion coatings improved the corrosion resistance of the HDGS due to the formation of silicate film. The addition of nano-silica improved the silicate networks and decreased the existing defects. The ratio of nano-silica / potassium silicate has been optimized in order to provide a high corrosion resistance. The results showed that, the corrosion resistance was improved with increasing silica ratio of silicate coatings. The film that formed with ratio 3 nano-silica is comparatively more protective and continuous. This can be related to the nano-silica particles size and the ability to fill the pores in potassium silicate coating.

In the present paper, a new method to form a dense silica layer onto galvanized steel was proposed, based on immersing of HDGS sheets immediately upon removing from the molten zinc in potassium silicate solution bath. One of the main aims of this study is to match some important industrial requirements concerning the deposition procedure, like low cost, small number of treatment steps and friendly to environment. Therefore, in the process presented in this paper, the silicate bath concentration and temperature of HDGS sheets upon removing from the molten zinc bath were optimized.

2. EXPERIMENTAL WORK

2.1. Sample Preparation

The samples were prepared by cutting steel sheet into 30×20×2 mm pieces. The chemical composition of the steel is listed in table 1. The samples were degreased for 2 min in a 10 g L^{-1} aqueous solution of Sodium hydroxide at 80°C and then rinsed with distilled water, pickled in a 10% Hydrochloric acid for 10 s, and then rinsed with distilled water. For galvanization the samples were fluxed in an aqueous solution containing 100 g L^{-1} of $ZnCl_2$ and 150 g L^{-1} of NH_4Cl at 60°C, dried and dipped into a molten zinc bath (prepared from zinc ingot consisting of 99.99% Zn) for 60 s at a temperature of 450°C, withdrawn at a constant speed, and then quenched immediately

upon removing from the molten zinc in Potassium silicate solution bath with chemical composition: 25% SiO_2 , 12% K_2O and 63% water, at metal immersion temperatures in excess of about 150°C. The immersion time was constant for 30 s. To optimize the operation process, different silicate bath concentrations: (1%, 2%, 4%, 6% and 8%) will be studied at three different temperatures of HDGS (150°C, 200°C and 250°C).

Table (1): Chemical composition of steel.

Fe	C	Si	Mn	P	S
Rent	0.23	0.045	0.14	0.035	0.03

2.2. Electrochemical Tests and Characterizations

Electrochemical tests were performed at 25°C using a Voltalab 40 Potentiostat (PGZ 301, Radiometer Analytical, France), in a conventional three-electrode cell, containing a reference electrode of Ag/AgCl, an auxiliary electrode of platinum wire and a piece of treated HDGS as the working electrode. The working electrodes were exposed (0.28 cm^2 area) to 3.5 wt.% aerated solution of Sodium chloride. Prior to the measurements, the working electrode was immersed in NaCl solution for 30 min to obtain a stable open-circuit potential (OCP).

The electrochemical impedance spectroscopy measurements (EIS) were carried out in a frequency range of 100 kHz to 50 mHz with amplitude of 10 mV peak-to-peak using ac signals at OCP. The Potentiodynamic polarization measurements were carried out at a scan rate of 2 mVs^{-1} in a range from -200 mV to +200 mV from OCP value. The impedance plots were fitted using the ZVIEW software.

Surface morphologies of the dried silicate-coated samples were observed by Scanning electron microscopy (SEM FEI INSPECT 50 S coupled with energy dispersion X-ray Analysis EDS Bruker AXS-Flash Detector 410-M) and the phase analysis was detected by X-rays diffraction (XRD PANalytical X'pert PRO.).

3. RESULTS AND DISCUSSION

3.1. Electrochemical Methods

3.1.1. Effect of silicate bath concentration

Figure 1 shows the Potentiodynamic polarization curves of HDGS with and without silicate treatment in 3.5 wt.% NaCl solution. Silicate coatings were obtained by 30 s immersion in different concentrations of potassium silicate solutions. Temperature of HDG steel sheets was kept constant at 250°C. The corresponding corrosion parameters such as corrosion current density (I_{corr}), corrosion potential (E_{corr}), cathodic slope (β_c), anodic slope (β_a) and polarization resistance (R_p) are listed in table 2. The polarization resistance is calculated by the equation (1) [40]:

$$R_p = \frac{\beta_a \times \beta_c}{2.303(\beta_a + \beta_c)} \times \frac{1}{I_{cor}} \quad \text{..... Eq. (1)}$$

As can be seen, R_p increased, and I_{corr} decreased in the presence of silicate coating in the order of 1% <2%< 4% <8%< 6% silicate concentration. Both the anodic and cathodic branches of the polarization curves of the silicate coating were observed in figure 1 which shift toward the direction where the corrosion current decreased, suggesting that the anodic process ($Zn \rightarrow Zn^{2+}+2e^-$) and the cathodic process ($O_2+2H_2O+4e^- \rightarrow 4OH^-$) of zinc corrosion were inhibited simultaneously. Therefore, the performance of these silicate coatings was dependent on their concentration. Corrosion resistance increase by increasing silicate concentration up to 6%, which is related to the formation of zinc-silicate complex at this concentration forming dense, compact and homogeneous layer at the surface. This can be confirmed by SEM-EDX analysis.

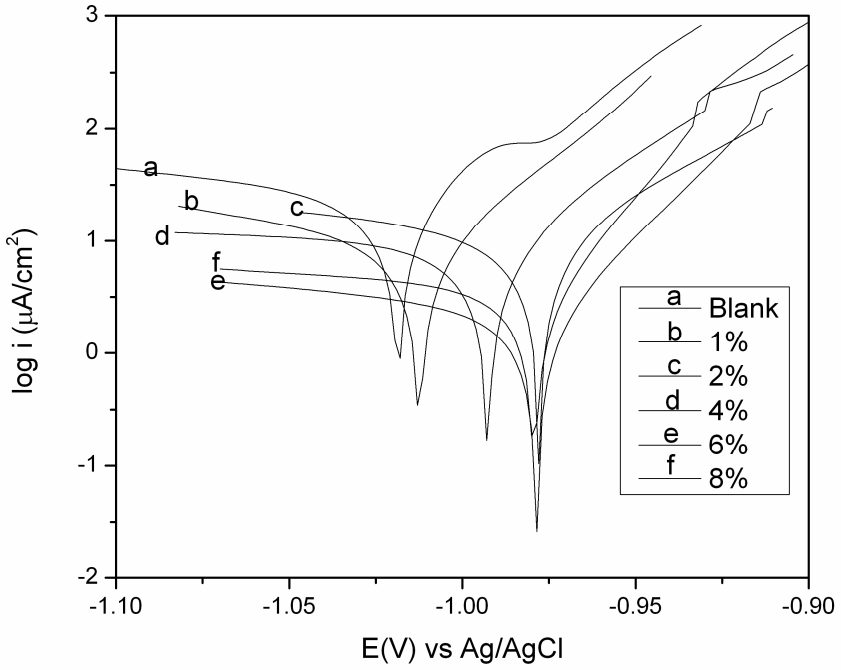

Fig. 1: Polarization curves of the silicate coatings of HDGS in 3.5 wt.% NaCl solution. Coatings were obtained from different concentrations of potassium silicate solution.

Table (2): Electrochemical parameters obtained from figure 1.

Sample	E_{corr} V vs. Ag/AgCl	R_p (kΩ· cm²)	I_{corr} (μA/ cm²)	β_a (V/dec)	β_c (V/dec)	Corr. Rate (μm/year)
Blank(HDG)	1.0187	0.76125	23.7581	56.1	301.8	277.8
1% silicate	1.0125	1.740	8.6395	45.3	185.6	101
2% silicate	0.9779	1.770	5.0497	40.5	85.7	59.07
4% silicate	0.9927	2.200	3.8216	33.2	85.6	44.69
6% silicate	0.9695	4.660	0.5089	26.9	99.7	22.97
8% silicate	0.9786	4.540	2.9228	34.1	317.1	26.8

EIS measurements were employed to confirm the anticorrosion behavior of the silicate coatings. Figures 2a & 2b show the Nyquist and Bode plots of silicate coated HDGS obtained by 30 s immersion in different silicate concentrations. EIS was measured at

OCP in 3.5 wt.% NaCl solution. The obtained Nyquist diagram consists of two depressed overlapping semicircles towards the real axis. The depressed semicircle in the low frequency region can be related to the combination of charge transfer resistance and the double layer capacitance. The high frequency semicircle was related to the resistance and capacitance of silicate coatings. To interpret these data, an appropriate equivalent circuit is proposed in figure 3, and the fitted results are listed in table 3.

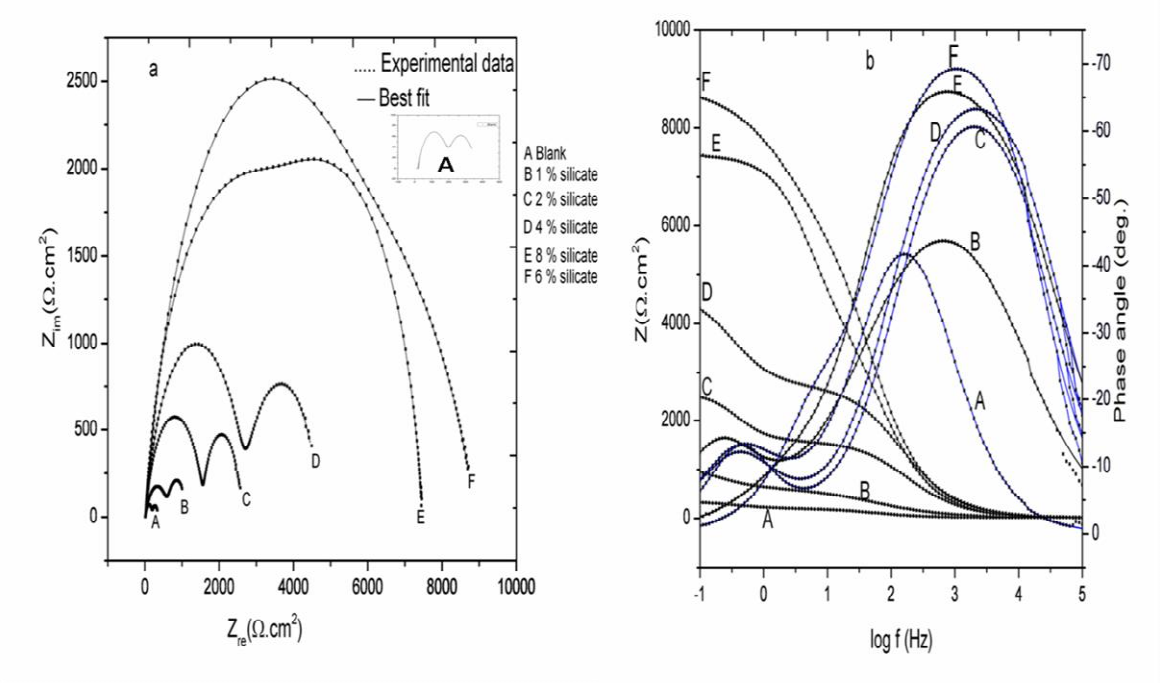

Fig. 2: (a) Nyquist plots and (b) Bode plots for the HDGS sample and the silicate coating samples, immersed in 3.5 wt.% NaCl solution.

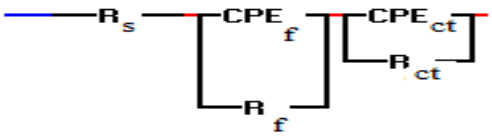

Fig. 3: Equivalent electrical circuit used for fitting EIS measurements.

In this equivalent circuit, R_s represents solution resistance, which is the ohmic resistance between the working and the reference electrode, while R_f and R_{ct} are the coating resistances and the charge transferee resistance, respectively. In case of the non-ideal behavior of the capacitance, it is necessary to replace the capacitors with the constant phase elements (CPE), where CPE_f and CPE_{ct} represent capacitance of the coating and capacitance of the substrate/coating interface (double layer capacitance), respectively. The most widely used explanation for the presence of CPE behavior and depressed semicircles on solid electrodes is the microscopic roughness, causing an inhomogeneous distribution in the solution resistance as well as in the double layer capacitance [41, 42]. P is the magnitude of the CPE and n is a factor that satisfies the condition $0 \leq n \leq 1$, which indicates how far (0), or how close (1), the interface is from being treated as an ideal capacitor. In the silicate-

coated samples, R_f corresponds to the silicate coating resistance, which mainly consisted of zinc oxides/hydroxides, zinc silicate [34] In the case of HDGS, R_f and R_{ct} could be related to the formation of the corrosion products composed of zinc oxides/hydroxychlorides, which can slightly inhibit the process of charge transfer [43]. As illustrated in table 3, the total impedance values (R_{ct}+ R_f) of the silicate-coated samples were higher than those of the HDGS sample, and with increasing silicate concentration, the coating resistance increased in the order of: 1% < 2% < 4% < 8% < 6%. This can be related to that silica treatment following the galvanizing process, which results in the addition of the silicon ions in the zinc coating to form a zinc-silicate complex, which is highly resistant to corrosion, and it would decrease the active area of the substrate. The formation of zinc-silicate complex will be confirmed by XRD analysis and SEM-EDX characterization, which will be discussed later.

Table (3): Fitted parameters for the HDGS samples with the silicate coatings using the equivalent circuit in figure 3.

Sample	R_s ($\Omega.cm^2$)	R_{ct} ($\Omega.cm^2$)	R_f ($\Omega.cm^2$)	P_{ct} ($\mu F.\ cm^{-2}$)	n_{ct}	P_f ($\mu F.\ cm^{-2}$)	n_f
HDG	20.834	176.99	158.61	7.6E-05	0.80948	0.00457	0.80979
1%	16.08	612.54	501.23	5.2E-05	0.64206	0.00242	0.83848
2%	18.105	1568.9	987.7	3.5E-06	0.79736	0.00055	0.94936
4%	19.058	2688.3	1989.3	2.4E-06	0.80112	0.00035	0.81366
6%	19.2	4655.7	4232.4	2.1E-06	0.86442	3.9E-05	0.62089
8%	21.1	3576.7	3866.7	2.2E-06	0.85112	1.5E-05	0.86183

3.1.2. Effect of immersed temperature of HDGS in silicate bath.

Corrosion behavior of HDGS sheets treated with 6% silicate concentration was investigated at three different temperatures of HDG steel sheets upon removing from molten zinc bath: 250°C, 200°C and 150°C.

Figure 4 presents the impedance diagrams of 6% silicate treated HDGS obtained at three different HDGS temperatures. EIS was measured at open circuit potential in 3.5% wt. NaCl solution. The impedance data showed two depressed capacitive loops, which are due to the conversion coatings and charge transfer resistances. The experimental data were fitted to equivalent circuit (figure 3) and the obtained values are listed in table 4. It can be seen that by increasing temperature of HDG steel sheets, the total impedance values (R_{ct}+ R_f) of the silicate-coated samples increased .This can be related to the formation of zinc – silicate complex which enhanced by increasing temperature of HDG steel.

Table (4): Fitted parameters using the equivalent circuit in figure 3 for the 6% silicate treatment at three different temperatures 250°C, 200°C and 150°C, immersed in 3.5 wt.% NaCl solution.

Sample	R_s ($\Omega.cm^2$)	R_{ct} ($\Omega.cm^2$)	R_f ($\Omega.cm^2$)	P_{ct} ($\mu F.\ cm^{-2}$)	n_{ct}	P_f ($\mu F.\ cm^{-2}$)	n_f
150°C	23.411	1135.2	2485.9	3.4E-05	0.92329	0.00042	0.94751
200°C	19.8	3608.5	3988	3.3E-05	0.9902	0.00032	0.81048
250°C	19.2	4655.7	4232.4	2.1E-06	0.86442	3.9E-05	0.62089

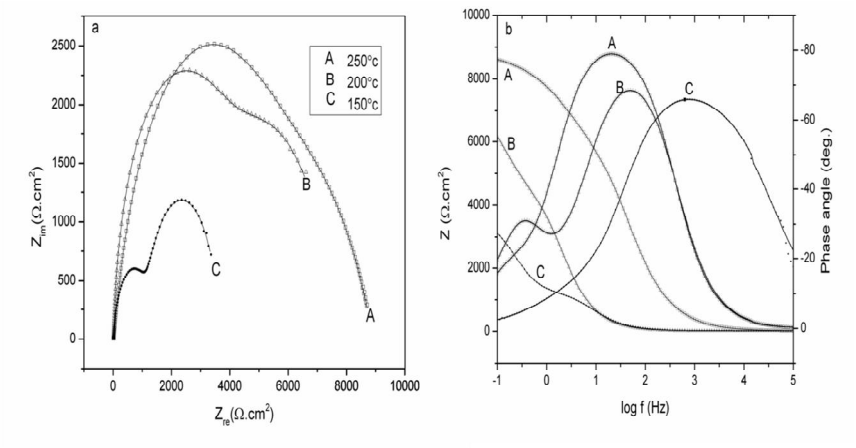

Fig. 4: (a) Nyquist plots and 4 (b) Bode plots for the 6% silicate treatment at three different temperatures 250°C, 200°C, 150°C, immersed in 3.5 wt.% NaCl solution.

As shown in figure 5, i_{corr} of tested samples decreases with increasing temperature of HDGS sheets. It may be realated to at elevated temperature the propability of formation of zinc-silicate complex increased, that gave higher corrsion resistance. Tafel parameters was listed in table 5.

Table (5): Electrochemical parameters obtained from figure 5.

Sample	E_{corr} (V) vs. Ag/Agcl	R_p (kΩ·cm^2)	I_{corr} (μA/cm^2)	β_a (V/dec)	β_c (V/dec)	Corr. Rate (μm/year)
150°C	-1.04	0.929	5.0119	30	16.7	58.60
200°C	-1.02	3.525	1.995	36	14.3	23.34
250°C	0.9695	4.660	0.5089	26.9	99.7	22.97

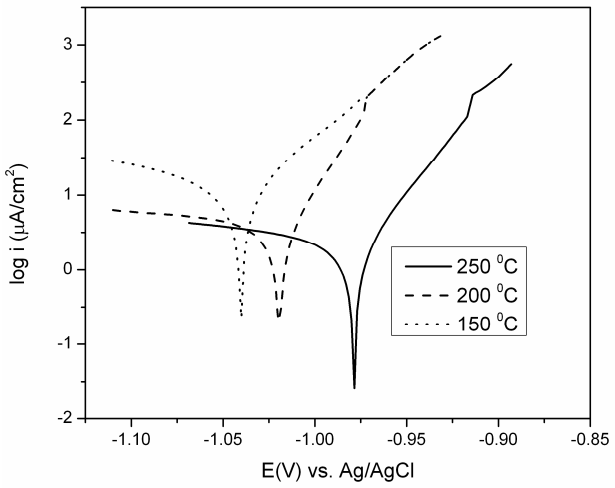

Fig. 5: Tafel plots of 6% silicate treated HDGS obtained at three different HDGS temperatures.

3.2. Surface Morphology and Characterization

The SEM technique was used to examine the surface morphology. Figures 6a and 6b show the SEM images HDGS and the potassium silicate conversion coating of HDGS obtained from potassium 6% silicate concentration at 250°C respectively.

The SEM observation showed that the silicate conversion coating was similar and resembled the HDG; the silicate coating has a homogeneous surface and is tightly anchored to the zinc coating. Table 6 lists the EDX results, it can be concluded that the percentage of silicon ions increased as the concentration of potassium silicate increased, confirming the formation of zinc-silicate complex.

The best corrosion resistance with 6% silicate concentration, but any further increasing in concentration more than 6%, will decrease the corrosion resistance, due to the formation of inhomogeneous coating and giving bad appearance.

Table (6): EDX analysis of the potassium silicate conversion coating of HDGS obtained from potassium silicate with different concentration at 250°C.

Sample	HDG	1% silicate	2% silicate	4% silicate	6% silicate	8% silicate
Si	Zero%	8.3%	9.63%	14.61%	22.94%	31.86%
Zn	92.7%	70.56%	75.83%	56.8%	47.36%	30.00%
O	7.3%	20.95%	14.54%	28.57%	29.7%	38.14%

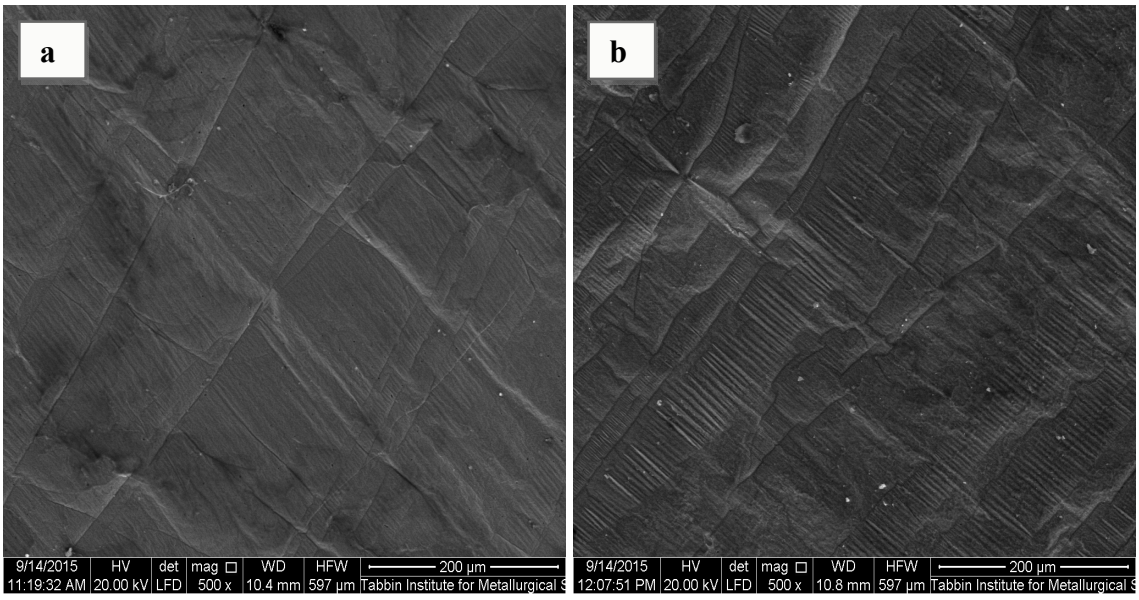

Fig. 6: SEM images of (a) HDGS and (b) potassium silicate conversion coated HDGS obtained from 6% potassium silicate 250°C.

Figures 7 a, b & c show the SEM images of the potassium silicate conversion coating of HDGS obtained from 6% potassium silicate concentration with different treatment temperatures of HDG steel sheets. The SEM observation showed that the treatment temperature affected the homogeneity of surface, and some areas were not covered on

the surface because of decreasing the temperature, which confirms that the formation of zinc – silicate complex increased as temperature increased since more silicon ions introduced to zinc layer [44]. EDS results listed in table 7, showed that as temperature increased the percentage of silicon in the layer increased, confirming that the formation of zinc- silicate complex increased as temperature increased.

Table (7): EDX analysis of the potassium silicate conversion coating of HDG obtained from 6% potassium silicate concentration with different temperatures.

Sample	250°C	200°C	150°C
Si	22.94%	14.99%	7.51%
Zn	47.36%	66.35%	75.37%
O	29.7%	18.38%	17.12%

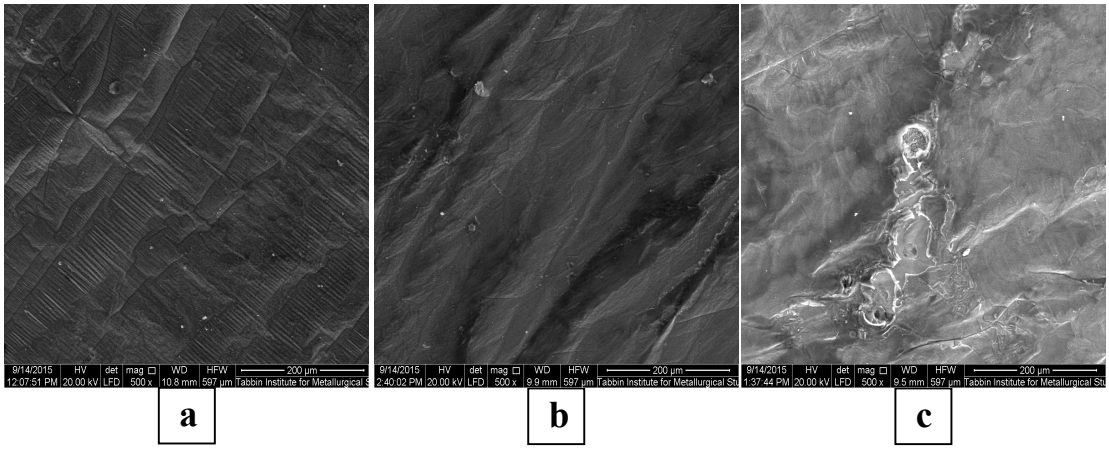

Fig. 7: SEM images of the potassium silicate conversion coating of HDG obtained from 6% potassium silicate concentration with different treatment temperatures of HDG steel sheets at treatment temperature (a) 250°C, (b) 200°C and (c) 150°C.

XRD analysis is an excellent tool to confirm the formation of zinc-silicate complex. Figure 8 shows the XRD pattern of HDGS and 6% and 8% silicate treated samples at 250°C temperature of HDGS. XRD pattern showed the presence of zinc-silicate complex in the treated samples (Zn_2SiO_4 phase, JCPDS card number 24-1469),and does not appeared in HDGS.

For further confirmation of the formation of zinc–silicate complex, A cross sectional SEM and EDS-mapping are shown in figures 9a to 9e, for potassium silicate conversion coating obtained from 6% silicate concentration at 250°C temperature of HDGS sheet, from the EDS analysis it can be concluded that the concentration of silicon ions gradually decreased from the surface to the bulk of sample, meaning that the concentration of silicon ions are higher near the surface and decreased gradually through the layers of the sample, as seen in table 8. Therefore, it can be concluded that the formation of zinc-silicate complex increased near the surface.

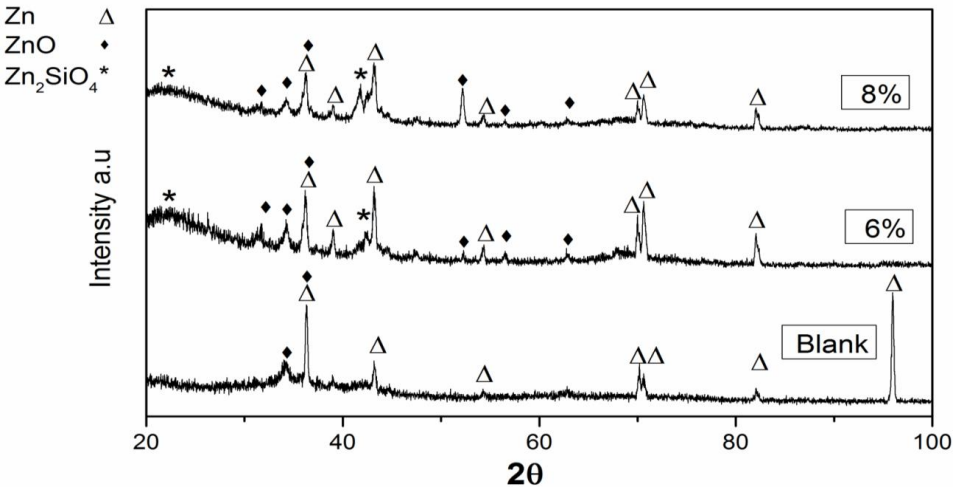

Fig. 8: XRD spectra of HDG (Blank) and 6% silicate treatment and 8% silicate treatment samples at 250°C.

Table (8): EDX cross-sectional analysis of the potassium silicate conversion coating of HDG obtained from 6% potassium silicate concentration at 250°C.

Point	Fe %	Zn %	Si %	O %
(1)	95.12	3.53	0.35	0
(2)	17.68	77.21	5.11	0
(3)	4.01	80.94	5.25	9.61
(4)	1.87	66.09	8.35	15.68

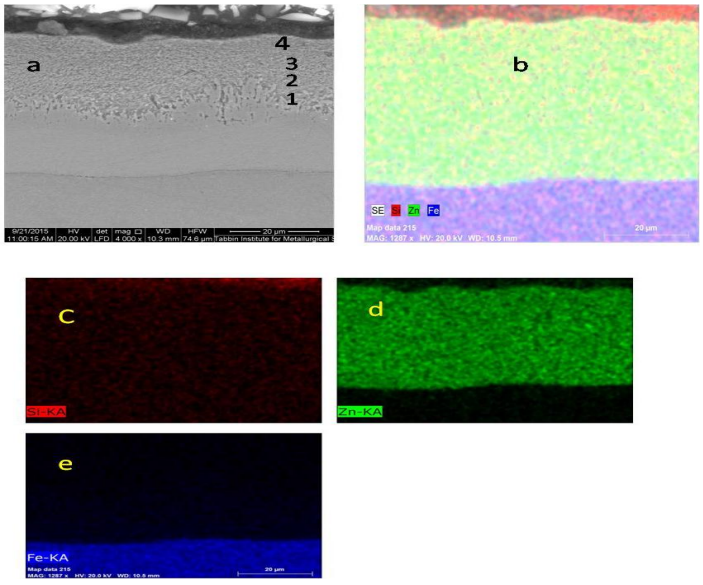

Fig. 9: (a) SEM image, (b) EDX cross-sectional mapping analysis and (c-e) EDX mapping of the potassium silicate conversion coating of HDG obtained from 6% potassium silicate concentration at 250°C.

4. CONCLUSION

- In conclusion, a method of inhibiting the corrosion of HDGS by subjecting the freshly zinc-coated metal to a treatment of potassium silicate at galvanizing temperatures was successfully achieved. The passivation treatment of HDGS by potassium silicate was investigated at different silicate concentration and different temperature of HDGS. The results of the electrochemical tests showed that in comparison to HDGS, the corrosion current densities of silicate coatings decreased, the polarization resistance and the total impedance values increased markedly, and the corrosion resistance was enhanced. The protective performance of the silicate coating is enhanced up to 6% silicate concentration and 250°C temperature of HDGS. The enhancement in corrosion resistance is related to the formation of zinc-silicate complex, which is highly resistance to corrosion, which was confirmed by the XED and EDX analysis.

5. REFERENCES

[1] Nürnberger, U.: "Long-time behavior of non-galvanized and galvanized steels for geotechnical stabilization applications". *MACO Materials and Corrosion,* vol. 63, pp. 1173-1180, (2012).

[2] Yang, W. J.; Yang, P.; Li, X. M. and Feng, W. L.: "Influence of tensile stress on corrosion behaviour of high-strength galvanized steel bridge wires in simulated acid rain". *Materials and Corrosion,* vol. 63, pp. 401-407, (2012).

[3] Bellezze, T.; Roventi, G.; Barbaresi, E.; Ruffini, N. and Fratesi, R.: "Effect of concrete carbonation process on the passivating products of galvanized steel reinforcements". *MACO Materials and Corrosion,* vol. 62, pp. 155-160, (2011).

[4] Kim, H.-J.; Zhang, J.; Yoon, R.-H. and Gandour, R.: "Development of environmentally friendly nonchrome conversion coating for electrogalvanized steel". *Surface and Coatings Technology,* vol. 188-189, pp. 762-767, (2004).

[5] LeBozec, N.; Thierry, D.; Peltola, A.; Luxem, L.; Luckeneder, G. and Marchiaro, G. *et al.*: "Corrosion performance of Zn-Mg-Al coated steel in accelerated corrosion tests used in the automotive industry and field exposures". *MACO Materials and Corrosion,* vol. 64, pp. 969-978, (2013).

[6] Veeraraghavan, B.; Haran, B.; Slavkov, D.; Prabhu, S.; Popov, B. and Heimann, B.: "Corrosion, passivation, and anodic films - development of a novel electrochemical method to deposit high corrosion resistant silicate layers on metal substrates". *Electrochemical and solid-state letters.,* vol. 6, p. B4, (2003).

[7] Hagans, P. L. and Haas, C. M.: "Influence of metallurgy on the protective mechanism of chromium-based conversion coatings on aluminum-copper alloys". *SIA Surface and Interface Analysis,* vol. 21, pp. 65-78, (1994).

[8] Twite, R. L. and Bierwagen, G. P.: "Review of alternatives to chromate for corrosion protection of aluminum aerospace alloys". *Progress in Organic Coatings,* vol. 33, pp. 91-100, (1998).

[9] Suda, A. and Asari, M.: "Behavior and mechanism of corrosion protection for galvanized steels by the self-healing effect of chromate coatings". *Corrosion engineerin.,* vol. 46, p. 111, (1997).

[10] Ramsey, J. D. and McCreery, R. L.: "In Situ Raman microscopy of chromate Effects on corrosion pits in aluminum alloy". *JOURNAL-ELECTROCHEMICAL SOCIETY,* vol. 146, pp. 4076-4081, (1999).

[11] Lin, B.-l. and Lu, J.-t.: "Self-healing mechanism of composite coatings obtained by phosphating and silicate sol post-sealing". *Transactions of Nonferrous Metals Society of China,* vol. 24, pp. 2723-2728, (2014).
[12] Su, H.-Y. and Lin, C.-S.: "Effect of additives on the properties of phosphate conversion coating on electrogalvanized steel sheet". *Corrosion Science,* vol. 83, pp. 137-146, (2014).
[13] Zhou, W. Q.; Sheng, L.; Xin, S. G.; Wang, J.; Kang, Y. H. and Wu, S. W.: "Effect of molybdate bath service life on corrosion resistance of conversion coating deposited on hot dip galvanized steel". *AMR Advanced Materials Research,* vol. 750-752, pp. 2012-2016, (2013).
[14] Lin, B. L.; Lu, J. T. and Kong, G.: "Effect of molybdate post-sealing on the corrosion resistance of zinc phosphate coatings on hot-dip galvanized steel". *Corrosion science.,* vol. 50, pp. 962-967, (2008).
[15] Ershov, S.; Druart, M. E.; Poelman, M.; Cossement, D.; Snyders, R. and Olivier, M. G.: "Deposition of cerium oxide thin films by reactive magnetron sputtering for the development of corrosion protective coatings". *Corrosion Science,* vol. 75, pp. 158-168, 10// (2013).
[16] Kong, G.; Liu, L.; Lu, J.; Che, C. and Zhong, Z.: "Study on lanthanum salt conversion coating modified with citric acid on hot dip galvanized steel". *Journal of Rare Earths,* vol. 28, pp. 461-465, 6// (2010).
[17] Kong, G.; Lingyan, L.; Lu, J.; Che, C. and Zhong, Z.: "Corrosion behavior of lanthanum-based conversion coating modified with citric acid on hot dip galvanized steel in aerated 1 M NaCl solution". *Corrosion Science,* vol. 53, pp. 1621-1626, 4// (2011).
[18] Dalbin, S.; Maurin, G.; Nogueira, R. P.; Persello, J. and Pommier, N.: "Silica-based coating for corrosion protection of electrogalvanized steel". *Surface and Coatings Technology,* vol. 194, pp. 363-371, 5/1/ (2005).
[19] Hara, M.; Ichino, R.; Okido, M. and Wada, N.: "Corrosion protection property of colloidal silicate film on galvanized steel". *Surface and Coatings Technology,* vol. 169-170, pp. 679-681, 6/2/ (2003).
[20] Jamali, F.; Danaee, I. and Zaarei, D.: "Effect of nano-silica on the corrosion behavior of silicate conversion coatings on hot-dip galvanized steel". *Materials and Corrosion,* vol. 66, pp. 459-464, (2015).
[21] Jiang, L.; Wolpers, M.; Volovitch, P. and Ogle, K.: "An atomic emission spectroelectrochemical study of passive film formation and dissolution on galvanized steel treated with silicate conversion coatings". *Surface and Coatings Technology,* vol. 206, pp. 3151-3157, 2/25/ (2012).
[22] Cole, J. A.; Roberts, W. O. and Turgeon, J. T.: "Method of protecting galvanized steel from corrosion". ed: Google Patents, (1991).
[23] Zhang, S. h.; Kong, G.; Sun, Z. w.; Che, C. s. and Lu, J. t.: "Effect of formulation of silica-based solution on corrosion resistance of silicate coating on hot-dip galvanized steel". *Surface and Interface Analysis,* (2016).
[24] Wang, R.-M.; Wang, J.-F.; Wang, X.-W.; He, Y.-F.; Zhu, Y.-F. and Jiang, M.-L.: "Preparation of acrylate-based copolymer emulsion and its humidity controlling mechanism in interior wall coatings". *Progress in Organic Coatings,* vol. 71, pp. 369-375, (2011).

[25] Kartsonakis, I.; Balaskas, A.; Koumoulos, E.; Charitidis, C. and Kordas, G.: "Incorporation of ceramic nanocontainers into epoxy coatings for the corrosion protection of hot dip galvanized steel". *Corrosion Science,* vol. 57, pp. 30-41, (2012).
[26] Brusciotti, F.; Batan, A.; Graeve, I. De; Wenkin, M.; Biessemans, M. and Willem, R. *et al.*: "Characterization of thin water-based silane pre-treatments on aluminium with the incorporation of nano-dispersed CeO_2 particles". *Surface and Coatings Technology,* vol. 205, pp. 603-613, (2010).
[27] Xue, D. and Van Ooij, W. J.: "Corrosion performance improvement of hot-dipped galvanized (HDG) steels by electro-deposition of epoxy-resin-ester modified bis-[tri-ethoxy-silyl] ethane (BTSE) coatings". *Progress in Organic Coatings,* vol. 76, pp. 1095-1102, (2013).
[28] Zhuravlev, L.: "The surface chemistry of amorphous silica. Zhuravlev model". *Colloids and Surfaces A: Physicochemical and Engineering Aspects,* vol. 173, pp. 1-38, (2000).
[29] Aramaki, K.: "Self-healing mechanism of an organosiloxane polymer film containing sodium silicate and cerium (III) nitrate for corrosion of scratched zinc surface in 0.5 M NaCl". *Corrosion Science,* vol. 44, pp. 1621-1632, (2002).
[30] Min, J.; Park, J. H.; Sohn, H.-K. and Park, J. M.: "Synergistic effect of potassium metal siliconate on silicate conversion coating for corrosion protection of galvanized steel". *Journal of Industrial and Engineering Chemistry,* vol. 18, pp. 655-660, (2012).
[31] Yuan, M.-r.; Lu, J.-t.; Kong, G. and Che, C.-s.: "Effect of silicate anion distribution in sodium silicate solution on silicate conversion coatings of hot-dip galvanized steels". *Surface and Coatings Technology,* vol. 205, pp. 4466-4470, (2011).
[32] Hara, M.; Ichino, R.; Okido, M. and Wada, N.: "Corrosion protection property of colloidal silicate film on galvanized steel". *Surface and Coatings Technology,* vol. 169, pp. 679-681, (2003).
[33] Dalbin, S.; Maurin, G.; Nogueira, R. P.; Persello, J. and Pommier, N.: "Silica-based coating for corrosion protection of electrogalvanized steel". *Surface and Coatings Technology,* vol. 194, pp. 363-371, (2005).
[34] Yuan, M.-r.; Lu, J.-t. and Kong, G.: "Effect of SiO_2: Na_2O molar ratio of sodium silicate on the corrosion resistance of silicate conversion coatings". *Surface and Coatings Technology,* vol. 204, pp. 1229-1235, (2010).
[35] Yuan, M.-r.; Lu, J.-t.; Kong, G. and Che, C.-s.: "Self healing ability of silicate conversion coatings on hot dip galvanized steels". *Surface and Coatings Technology,* vol. 205, pp. 4507-4513, (2011).
[36] Jamali,F.; Danaee, I. and Zaarei, D.: "Effect of nano-silica on the corrosion behavior of silicate conversion coatings on hot-dip galvanized steel". *Materials and Corrosion,* vol. 66, pp. 459-464, (2015).
[37] Veeraraghavan, B.; Slavkov, D.; Prabhu, S.; Nicholson, M.; Haran, B. and Popov, B. *et al.*: "Synthesis and characterization of a novel non-chrome electrolytic surface treatment process to protect zinc coatings". *Surface and Coatings Technology,* vol. 167, pp. 41-51, (2003).
[38] Aramaki, K.: "The inhibition effects of chromate-free, anion inhibitors on corrosion of zinc in aerated 0.5 M NaCl". *Corrosion Science,* vol. 43, pp. 591-604, (2001).
[39] Parashar, G.; Bajpayee, M. and Kamani, P.: "Water-borne non-toxic high-performance inorganic silicate coatings". *Surface Coatings International Part B: Coatings Transactions,* vol. 86, pp. 209-216, (2003).

[40] Danaee, I.; Ghasemi, O.; Rashed, G.; Avei, M. R. and Maddahy, M.: "Effect of hydroxyl group position on adsorption behavior and corrosion inhibition of hydroxybenzaldehyde Schiff bases: Electrochemical and quantum calculations". *Journal of Molecular Structure,* vol. 1035, pp. 247-259, (2013).
[41] Danaee, I. and Noori, S.: "Kinetics of the hydrogen evolution reaction on NiMn graphite modified electrode". *International journal of hydrogen energy,* vol. 36, pp. 12102-12111, (2011).
[42] Danaee, I.; Khomami, M. N. and Attar, A.: "Corrosion behavior of AISI 4130 steel alloy in ethylene glycol–water mixture in presence of molybdate". *Materials Chemistry and Physics,* vol. 135, pp. 658-667, (2012).
[43] Lin, B.-l.; Lu, J.-t. and Kong, G.: "Synergistic corrosion protection for galvanized steel by phosphating and sodium silicate post-sealing". *Surface and Coatings Technology,* vol. 202, pp. 1831-1838, (2008).
[44] Cole, J. A.; Roberts, W. O. and Turgeon, J. T.: "Coating metal with molten zinc or its alloys reacted with silica compound". ed: Google Patents, (1991).